

OBSERVED BEHAVIOR OF HIGHLY INELASTIC
ELECTRON-PROTON SCATTERING

M. Breidenbach, J. I. Friedman, H. W. Kendall

Department of Physics and Laboratory for Nuclear Science,*
Massachusetts Institute of Technology, Cambridge, Massachusetts 02139

E. D. Bloom, D. H. Coward, H. DeStaeblcr,
J. Drees, L. W. Mo, R. E. Taylor

Stanford Linear Accelerator Center, † Stanford, California 94305

ABSTRACT

The results of the SLAC-MIT electron-proton inelastic scattering experiment at 6° and 10° are discussed. Although the kinematic range of these measurements is insufficient to separate the structure functions W_1 and W_2 , estimates of W_2 can be obtained. If the interaction is dominated by transverse virtual photons, W_2 can be expressed as a function of $\omega = 2M\nu/q^2$ within experimental errors for $q^2 > 1$ and $\omega > 4$, where ν is the invariant energy transfer and q^2 is the invariant momentum transfer of the electron. Various theoretical models are briefly discussed, and the predictions of several sum rules are compared with the data.

*Work supported in part through funds provided by the Atomic Energy Commission under Contract No. AT(30-1)2098.

†Supported by the U. S. Atomic Energy Commission.

In a previous letter,¹ we have reported experimental results from a SLAC-MIT study of high energy inelastic electron proton scattering. Measurements of inelastic spectra, in which only the scattered electrons were detected, were made at scattering angles of 6° and 10° and with incident energies between 7 and 17 GeV. In this communication, we discuss some of the salient features of inelastic spectra in the deep continuum region.

One of the interesting features of the measurements is the weak momentum transfer dependence of the inelastic cross sections for excitations well beyond the resonance region. This weak dependence is illustrated in Fig. 1. Here we have plotted the differential cross section divided by the Mott cross section, $(d^2\sigma/d\Omega dE')/(d\sigma/d\Omega)_{\text{MOTT}}$, as a function of the square of the four-momentum transfer, $q^2 = 2EE'(1 - \cos\theta)$, for constant values of the invariant mass of the recoiling target system, W , where $W^2 = 2M(E - E') + M^2 - q^2$. E is the energy of the incident electron, E' is the energy of the final electron, and θ is the scattering angle, all defined in the laboratory system; M is the mass of the proton. The cross section is divided by the Mott cross section

$$\left(\frac{d\sigma}{d\Omega}\right)_{\text{MOTT}} = \frac{e^4}{4E^2} \frac{\cos^2\theta/2}{\sin^4\theta/2}$$

in order to remove the major part of the well-known four-momentum transfer dependence arising from the photon propagator. Results from both 6° and 10° are included in the figure for each value of W . As W increases, the q^2 dependence appears to decrease. The striking difference between the behavior of the inelastic and elastic cross sections is also illustrated in Fig. 1, where the elastic cross section, divided by the Mott cross section for $\theta = 10^\circ$, is included. The q^2 dependence of the deep continuum is also considerably weaker than that of the electro-excitation of the resonances,² which have a q^2 dependence similar to that of elastic scattering for $q^2 > 1(\text{GeV}/c)^2$.

On the basis of general considerations, the differential cross section for inelastic electron scattering, in which only the electron is detected, can be represented by the following expression³:

$$\frac{d^2\sigma}{d\Omega dE'} = \left(\frac{d\sigma}{d\Omega}\right)_{\text{MOTT}} \left[W_2 + 2W_1 \tan^2 \theta/2 \right].$$

The form factors, W_2 and W_1 , depend on the properties of the target system, and can be represented as functions of q^2 and $\nu = E - E'$, the electron energy loss. The ratio, W_2/W_1 , is given by

$$W_2/W_1 = \left(\frac{q^2}{\nu^2 + q^2} \right) (1 + R) \quad R \geq 0 ,$$

where R is the ratio of the photo-absorption cross sections of longitudinal and transverse virtual photons, $R = \sigma_S/\sigma_T$.⁴

The objective of our investigations is to study the behavior of W_1 and W_2 to obtain information about the structure of the proton and its electromagnetic interactions at high energies. Since at present only cross-section measurements at small angles are available, we are unable to make separate determinations of W_2 and W_1 . However, we can place limits on W_2 and study the behavior of these limits as a function of the invariants, ν and q^2 .

Bjorken⁵ originally suggested that W_2 could have the form

$$W_2 = \frac{1}{\nu} F(\omega)$$

where

$$\omega = 2M\nu/q^2 .$$

$F(\omega)$ is a universal function that is conjectured to be valid for large values of ν and q^2 . This function is universal in the sense that it manifests scale invariance, that is, it depends only on the ratio ν/q^2 .

Since

$$\nu W_2 = \frac{\nu \frac{d^2\sigma}{d\Omega dE'}}{(\frac{d\sigma}{d\Omega})_{\text{MOTT}}} \left[1 + 2 \frac{1}{1+R} (1 + \nu^2/q^2) \tan^2 \theta/2 \right]^{-1},$$

the value of νW_2 for any given measurement clearly depends on the presently unknown value of R . It should be noted that the sensitivity to R is small when $2(1 + \nu^2/q^2) \tan^2 \theta/2 \ll 1$. Experimental limits on νW_2 can be calculated on the basis of the extreme assumptions $R=0$ and $R=\infty$. In Fig. 2A and 2B the experimental values of νW_2 from the 6° and 10° data for $q^2 > 0.5 (\text{GeV}/c)^2$ are shown as a function of ω for the assumption that $R=0$. Figures 2C and 2D show the experimental values of νW_2 calculated from the 6° and 10° data with $q^2 > 0.5 (\text{GeV}/c)^2$ under the assumption $R=\infty$. The 6° , 7 GeV results for νW_2 , all of which have values of $q^2 \leq 0.5 (\text{GeV}/c)^2$, are shown for both assumptions in Fig. 2E. The elastic peaks are not displayed in Fig. 2.

The results shown in these figures indicate the following:

(1) If $\sigma_T \gg \sigma_S$, the experimental results are consistent with a universal curve for $\omega \gtrsim 4$ and $q^2 \gtrsim .5 (\text{GeV}/c)^2$. Above these values, the measurements at 6° and 10° give the same results within the errors of measurements. The 6° , 7 GeV measurements of νW_2 , all of which have values of $q^2 \leq 0.5 (\text{GeV}/c)^2$, are somewhat smaller than the results from the other spectra in the continuum region.

The values of νW_2 for $\omega \gtrsim 5$ show a gradual decrease as ω increases. In order to test the statistical significance of the observed slope, we have made linear least squares fits to the values of νW_2 in the region $6 \leq \omega \lesssim 25$. These fits give $\nu W_2 = (0.351 \pm .023) - (.00386 \pm .00088) \omega$ for data with $q^2 > 0.5 (\text{GeV}/c)^2$ and $\nu W_2 = (0.366 \pm .024) - (.0045 \pm .0019) \omega$ for $q^2 > 1 (\text{GeV}/c)^2$. The quoted errors consist of the errors from the fit added in quadrature with estimates of systematic errors.

Since $\sigma_T + \sigma_S \simeq 4\pi^2 \alpha \left(\frac{\nu W_2}{q^2} \right)$ for $\omega \gg 1$, our results can provide information about the behavior of σ_T if $\sigma_T \gg \sigma_S$. The scale invariance found in the measurements of νW_2 indicates that the q^2 dependence of σ_T is approximately $1/q^2$. The gradual decrease exhibited in νW_2 for large ω suggests that the photo absorption cross section for virtual photons falls slowly at constant q^2 as the photon energy ν increases.

The measurements indicate that νW_2 has a broad maximum in the neighborhood of $\omega = 5$. The question of whether this maximum has any correspondence to a possible quasi-elastic peak⁷ requires further investigation.

It should be emphasized that all of the above conclusions are based on the assumption that $\sigma_T \gg \sigma_S$.

(2) If $\sigma_S \gg \sigma_T$, the measurements of νW_2 do not follow a universal curve and have the general feature that at constant $2M\nu/q^2$, the value of νW_2 increases with q^2 .

(3) For either assumption, νW_2 shows a threshold behavior in the range $1 \leq \omega \lesssim 4$. W_2 is constrained to be zero at inelastic threshold which corresponds to $\omega \simeq 1$ for large q^2 . In the threshold region of νW_2 , W_2 falls rapidly as q^2 increases at constant ν . This is qualitatively different from the weak q^2 behavior for $\omega > 4$. For $q^2 \gtrsim 1 (\text{GeV}/c)^2$, the threshold region contains the resonances excited in electroproduction. As q^2 increases, the variations due to these resonances damp out and the values of νW_2 do not appear to vary rapidly with q^2 at constant ω .

It can be seen from a comparison of Fig. 2A and 2C that the 6^0 data provide a measurement of νW_2 to within 10% up to a value of $\omega \approx 6$, irrespective of the values of R .

There have been a number of different theoretical approaches in the interpretation of the high-energy inelastic electron scattering results. One class of

models,⁶⁻⁹ referred to as parton models, describes the electron as scattering incoherently from point-like constituents within the proton. Such models lead to a universal form for νW_2 , and the point charges assumed in specific models give the magnitude of νW_2 for $\omega > 2$ to within a factor of two.⁷ Another approach¹⁰⁻¹¹ relates the inelastic scattering to off-the-mass-shell Compton scattering which is described in terms of Regge exchange using the Pommeranchuk trajectory. Such models lead to a flat behavior of νW_2 as a function of ν but do not require the weak q^2 dependence observed and do not make any numerical predictions at this time. Perhaps the most detailed predictions made at present come from a vector dominance model which primarily utilizes the ρ meson.¹² This model reproduces the gross behavior of the data and has the feature that νW_2 asymptotically approaches a function of ω as $q^2 \rightarrow \infty$. However, a comparison of this model with the data leads to statistically significant discrepancies. This can be seen by noting that the prediction for $d^2\sigma/d\Omega dE'$ contains a parameter ξ , the ratio of the cross sections for longitudinally and transversely polarized ρ mesons on protons, which is expected to be a function of W but which should be independent of q^2 . For values of $W \geq 2$ GeV, the experimental values of ξ increase by about $(50 \pm 5)\%$ as q^2 increases from 1 to 4 $(\text{GeV}/c)^2$. This model predicts that

$$\sigma_S/\sigma_T = \xi(K) \frac{q^2}{m_\rho^2} \left[1 - q^2/2m_\rho \nu \right],$$

which will provide the most stringent test of this approach when a separation of W_1 and W_2 can be made.

The application of current algebra¹³⁻¹⁷ and the use of current commutators leading to sum rules and sum rule inequalities provide another way of comparing the measurements with theory. There have been some recent theoretical considerations¹⁸⁻²⁰ which have pointed to possible ambiguity in these calculations; however, it is still of considerable interest to compare them with experiment.

In general, W_2 and W_1 can be related to commutators of electromagnetic current densities.^{5,16} The experimental value of the energy-weighted sum $\int_1^\infty \frac{d\omega}{\omega} (\nu W_2)$, which is related to the equal time commutator of the current and its time derivative, is 0.16 ± 0.01 for $R = 0$ and 0.20 ± 0.03 for $R = \infty$. The integral has been evaluated with an upper limit $\omega = 20$. This integral is also important in parton theories where its value is the mean square charge per parton.

Gottfried²¹ has calculated a constant q^2 sum rule for inelastic electron-proton scattering based on a non-relativistic quark model involving point-like quarks. The resulting sum rule is:

$$\int_1^\infty \frac{d\omega}{\omega} (\nu W_2) = \int_{q^2/2M}^\infty d\nu W_2 = 1 - \frac{G_{Ep}^2 + q^2/4M^2 G_{Mp}^2}{1 + q^2/4M^2}$$

where G_{Ep} and G_{Mp} are the electric and magnetic form factors of the proton. The experimental evaluation of this integral from our data is much more dependent on the assumption about R than the previous integral. We will thus use the 6° measurements of W_2 which are relatively insensitive to R . Our data for a value of $q^2 \simeq 1 \text{ (GeV/c)}^2$, which extends to a value of ν of about 10 GeV, gives a sum that is 0.72 ± 0.05 with the assumption that $R = 0$. For $R = \infty$, its value is $0.81 \pm .06$. An extrapolation of our measurements of νW_2 for each assumption suggests that the sum is saturated in the region $\nu \simeq 20 - 40$ GeV. Bjorken¹³ has proposed a constant q^2 sum rule inequality for high energy scattering from the proton and neutron derived on the basis of current algebra. His result states that

$$\int_1^\infty \frac{d\omega}{\omega} \nu [W_{2p} + W_{2n}] = \int_{q^2/2M}^\infty d\nu [W_{2p} + W_{2n}] \geq \frac{1}{2}$$

where the subscripts p and n refer to the proton and neutron respectively. Since there are presently no electron-neutron inelastic scattering results available, we estimate W_{2n} in a model-dependent way. For a quark model²² of the proton, $W_{2n} \simeq 0.8 W_{2p}$ whereas in the model⁸ of Drell and co-workers, W_{2n} rapidly approaches W_{2p} as ν increases. Using our results, this inequality is just satisfied at $\omega \simeq 4.5$ for the quark model and at $\omega \simeq 4.0$ for the other model for either assumption about R. For example, this corresponds to a value of $\nu \simeq 4.5$ GeV for $q^2 = 2$ (GeV/c)². Bjorken²³ estimates that the experimental value of the sum is too small by about a factor of two for either model, but it should be noted that the q^2 dependence found in the data is consistent with the predictions of this calculation.

REFERENCES

1. E. Bloom et al., Report No. SLAC-PUB-642, Stanford Linear Accelerator Center, Stanford University, Stanford, California (1969) (to be published).
2. Preliminary results from the present experimental program are given in the report by W.K.H. Panofsky in the Proceedings of the XIVth Internl. Conf. On High Energy Physics, Vienna, Austria (1968). (CERN Scientific Information Service, Geneva, Switzerland, 1968.)
3. R. von Gehlen, Phys. Rev. 118, 1455 (1960); J. D. Bjorken (1960), unpublished; M. Gourdin, Nuovo Cimento 21, 1094 (1961).
4. See L. Hand, Proceedings of the 1967 Symposium on Electron and Photon Interactions at High Energies, or F. J. Gilman, Phys. Rev. 167, 1365 (1968).
5. J. D. Bjorken, Phys. Rev. 179, 1547 (1969).
6. R. P. Feynman (private communication).
7. J. D. Bjorken and E. A. Paschos, Report No. SLAC-PUB-572, Stanford Linear Accelerator Center, Stanford University, Stanford, California (1969) (to be published).
8. S. J. Drell, D. J. Levy, and T. M. Yan, Phys. Rev. Letters 22, 744 (1969).
9. K. Huang, Proceedings of the Symposium on Multiparticle Production, ANL 150 (1968).
10. H. D. Abarbanel, M. L. Goldberger, Phys. Rev. Letters 22, 500 (1969).
11. H. Harari, Phys. Rev. Letters 22, 1078 (1969).
12. J. J. Sakurai, Phys. Rev. Letters 22, 981 (1969).
13. J. D. Bjorken, Phys. Rev. Letters 16, 408 (1966).
14. J. D. Bjorken, Proceedings of Internl. School of Physics "Enrico Fermi," Varenna, 55 (1967).

15. J. M. Cornwall and R. E. Norton, Phys. Rev. 177, 2584 (1969).
16. C. G. Callan, Jr., and D. J. Gross, Phys. Rev. Letters 21, 311 (1968).
17. C. G. Callan, Jr., and D. J. Gross, Phys. Rev. Letters 22, 156 (1969).
18. R. Jackiw and G. Preparata, Phys. Rev. Letters 22, 975 (1969).
19. S. L. Adler and Wu-Ki Tung, Phys. Rev. Letters 22, 978 (1969).
20. H. Cheng and T. S. Wu, Phys. Rev. Letters 22, 1409 (1969).
21. Kurt Gottfried, Phys. Rev. Letters 18, 1174 (1967).
22. J. D. Bjorken, Report No. SLAC-PUB-571, Stanford Linear Accelerator Center, Stanford University, Stanford, California (1969).
23. J. D. Bjorken (private communication).

Figure Captions

1. $(d^2\sigma/d\Omega dE')/\sigma_{\text{MOTT}}$ vs q^2 for $W = 2, 3,$ and 3.5 GeV in GeV^{-1} .
 The lines drawn through the data are meant to guide the eye. Also shown is the cross section for elastic e-p scattering, divided by σ_{MOTT} , $(d\sigma/d\Omega)/\sigma_{\text{MOTT}}$, calculated for $\theta = 10^\circ$, using the dipole form factor. The relatively slow variation with q^2 of the inelastic cross section compared with the elastic cross section is clearly shown.
2. νW_2 vs $\omega = 2M\nu/q^2$ is shown for various assumptions about $R = \sigma_S/\sigma_T$.
 (a) 6° data except for 7-GeV spectrum for $R = 0$. (b) 10° data for $R = 0$.
 (c) 6° data except for 7-GeV spectrum for $R = \infty$, (d) 10° data for $R = \infty$.
 (e) 6° , 7-GeV spectrum for $R = 0$ and $R = \infty$.

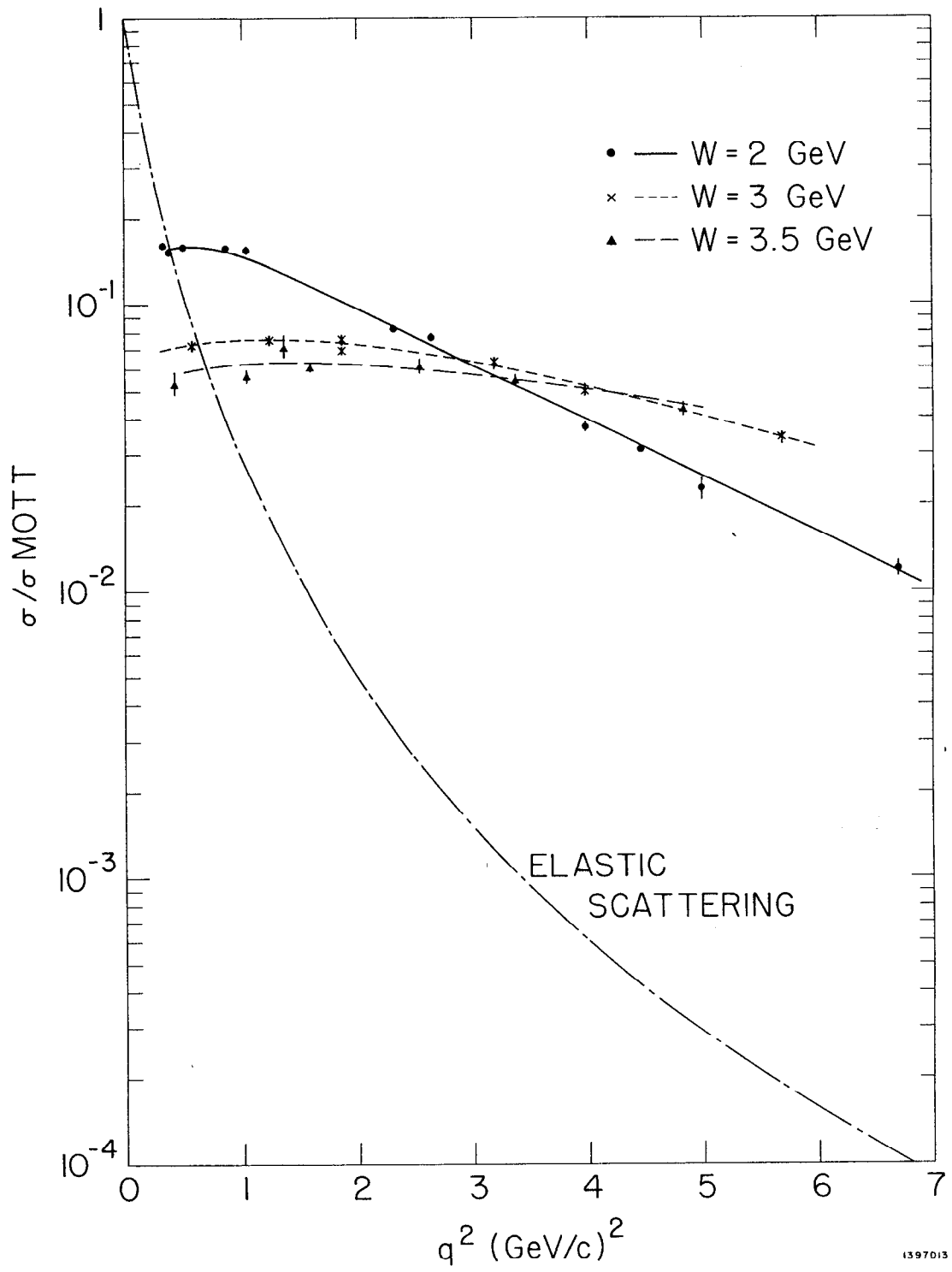


Fig. 1

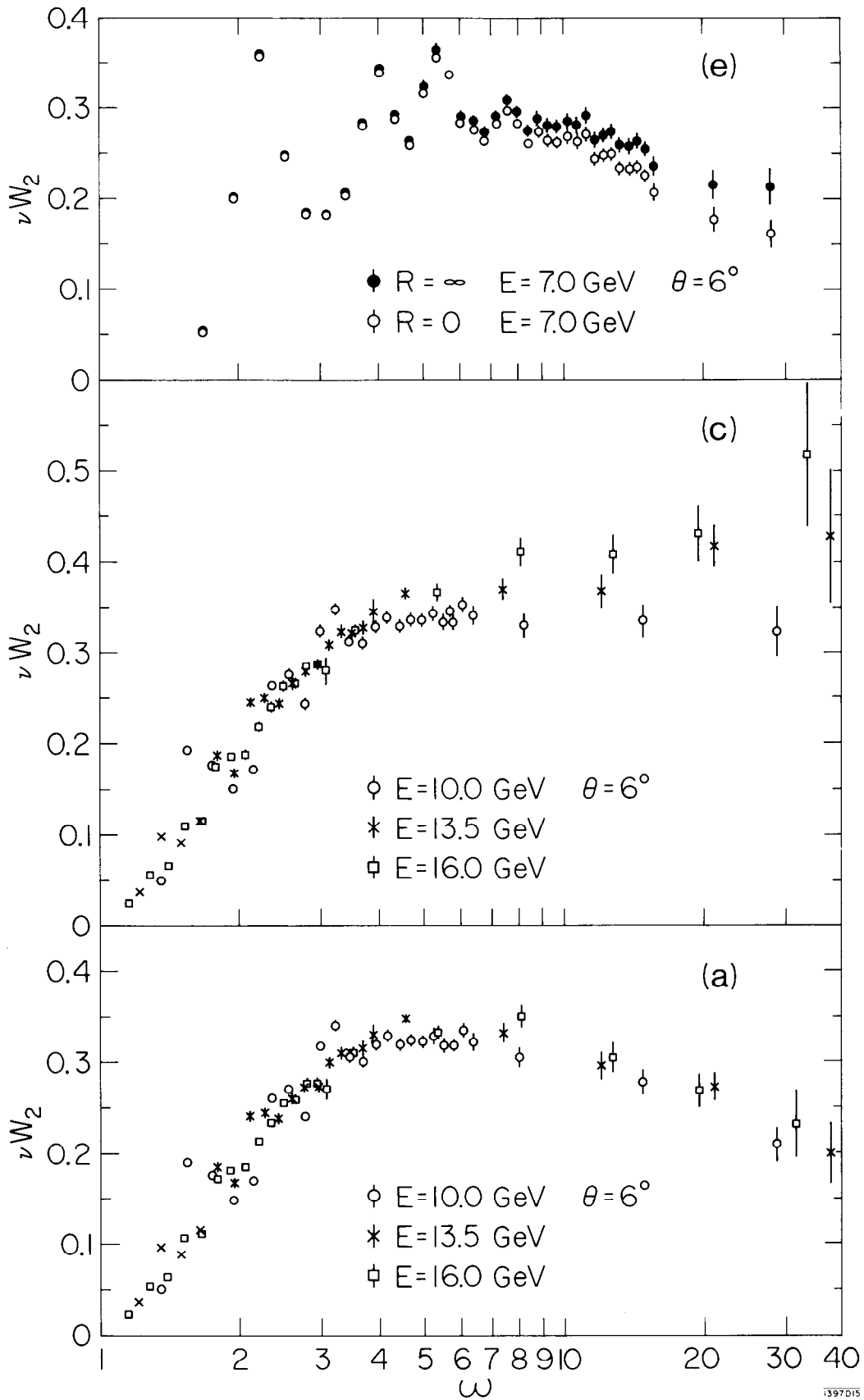


Fig. 2a, 2c, 2e

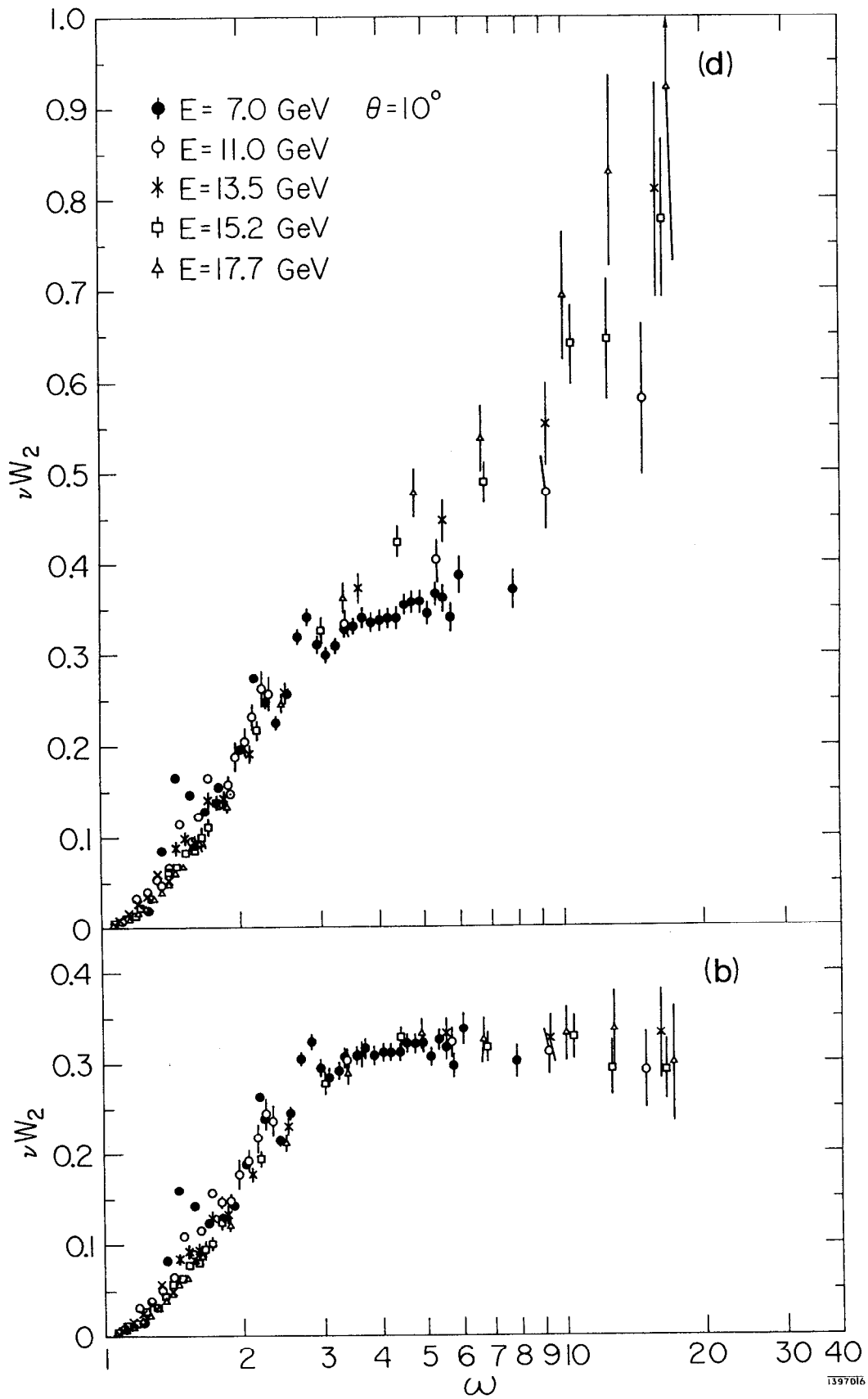


Fig. 2b,2d